IEEE Access
Multidisciplinary ⋮ Rapid Review ⋮ Open Access Journal

Received 29 May 2024, accepted 12 June 2024, date of publication 17 June 2024, date of current version 26 June 2024.

Digital Object Identifier 10.1109/ACCESS.2024.3415478

RESEARCH ARTICLE

Scalable Neural Dynamic Equivalence for Power Systems

QING SHEN[1], (Graduate Student Member, IEEE), YIFAN ZHOU[1], (Member, IEEE), PENG ZHANG[1], HUANFENG ZHAO[1], (Member, IEEE), QIANG ZHANG[2], (Senior Member, IEEE), SLAVA MASLENNIKOV[2], (Senior Member, IEEE), AND XIAOCHUAN LUO[2], (Senior Member, IEEE)

[1]Department of Electrical and Computer Engineering, Stony Brook University, Stony Brook, NY 11790, USA
[2]ISO New England Inc., Holyoke, MA 01040, USA

Corresponding author: Yifan Zhou (yifan.zhou.1@stonybrook.edu)

This work was supported in part by the National Science Foundation under Grant No. ITE-2134840. This work relates to Department of Navy award N00014-24-1-2287 issued by the Office of Naval Research. The U.S. Government has a royalty-free license throughout the world in all copyrightable material contained herein.

ABSTRACT Traditional grid analytics heavily rely on accurate power system models, especially dynamic ones for generators, controllers, and loads. However, obtaining comprehensive models is impractical in real operations due to inaccessible parameters and consumer privacy. This necessitates dynamic equivalencing for unknown subsystems, which employs physics-informed machine learning and neural ordinary differential equations (ODE-NET) to preserve dynamic behaviors post-disturbances. The contributions include: 1) A neural dynamic equivalence (NeuDyE) formulation enabling continuous-time, data-driven dynamic equivalence, eliminating the need for acquiring inaccessible system details; 2) Introduction of Physics-Informed NeuDyE learning (PI-NeuDyE) to actively control NeuDyE's closed-loop accuracy; 3) Driving Port NeuDyE (DP-NeuDyE), a practical application of NeuDyE, reducing the number of inputs required for training. Extensive case studies on the 140-bus NPCC system validate the generalizability and accuracy of both PI-NeuDyE and DP-NeuDyE. These analyses cover various scenarios, including limitations in data accessibility. Test results demonstrate the scalability and practicality of NeuDyE, showcasing its potential application in ISO and utility control centers for online transient stability analysis and planning purposes.

INDEX TERMS Neural dynamic equivalence, ODE-NET, physics-informed machine learning, model order reduction, driving port.

I. INTRODUCTION

Reliable discovery of dynamic equivalent models for unidentified subsystems, especially external systems, is crucial to ensure reliable operations of large-scale interconnected transmission systems [1]. This task has been a longstanding challenge due to the existence of nonlinear dynamics, complex coherency characteristics, and unavailable component models in power systems [2], [3]. Recent advancements in Phasor Measurement Units (PMUs) provide an opportunity to readily obtain a rich history of high-data-rate measurements, which fostered the development of data-driven dynamic equivalence using machine learning techniques [4]. While the utilization of neural networks in power systems is not a new concept [11], [12], their application in power system dynamic equivalence remains an evolving area of research [7], [13]. Early investigations primarily concentrated on the direct application of neural networks in power system analysis [16], [17] or the use of deep learning methods to unveil power system dynamics. Examples include employing recurrent neural networks for predicting dynamic variations [18], [19] and designing convolutional neural networks for stability assessment [20], [21]. Some studies in dynamic modeling utilize the Koopman operator framework [24], mapping nonlinear systems into higher-dimensional linear representations. However, the computational complexity associated with mapping large-scale systems to an even higher dimension is substantial. Identification and parameter

The associate editor coordinating the review of this manuscript and approving it for publication was Atri Bera.

estimation methods, as outlined in [31], can be employed to determine the unknown parameters of the dynamic equivalent model. Another approach is the frequency-scanning-based impedance modeling [30], whereas the equivalent model is a linear dynamic system that proves effective solely at a single operating point, rendering it unable to capture transients during faults. Distinguished from these methods, Physics-Informed Neural Networks (PINNs) are engineered to directly leverage physical knowledge to assist the training procedure [22]. For example, a specialized PINN is designed for Differential Algebraic Equations (DAEs), which can simulate both state and algebraic variables for well-established power system test cases [23].

Despite various attempts being reported in the literature, significant challenges persist. First, learning continuous-time dynamic behaviors using discrete-time measurements poses a considerable obstacle. Traditional discretization techniques may not fully capture the intricacies of the continuous dynamics, leading to large inaccuracies that limit their practical implementations. Second, achieving robust and stable closed-loop operations under diverse operating conditions and disturbances is essential for safe plug-and-play integration of dynamic equivalence.

This paper makes three contributions to address the aforementioned challenges:

- Formulation of Ordinary Differential Equations (ODEs)-Net-enabled Dynamic Equivalence (NeuDyE): This approach leverages ODEs and neural networks to model the system dynamics accurately, providing a data-driven representation that aligns with the continuous-time behavior of power grids.
- Introduction of Physics-Informed Neural Dynamic Equivalence (PI-NeuDyE): It combines an ODE-NET-enabled equivalent model with physics-informed learning to identify a continuous-time dynamic equivalence while ensuring a controllable alignment in the closed-loop dynamic behaviors under disturbances.
- Implementation of a Driving Port NeuDyE (DP-NeuDyE): It reduces the number of inputs required for training, making the method more manageable and cost-effective to deploy in real-world interconnected bulk power systems.
- An extensive comparative analysis is conducted to discuss the pros and cons of PI-NeuDyE and DP-NeuDyE.

This article is organized as follows: Section II introduces the mathematical basis of NeuDyE, i.e., how to formulate and simulate a power system with subsystems modeled by neural dynamic equivalence. Section III explains the key technology of PI-NeuDyE, which is to use Neural-Ordinary-Differential-Equation-Network (ODE-NET) to discover the dynamic equivalence of power systems. Section IV introduces a variant of NeuDyE called DP-NeuDyE to further trim the features needed. Section V presents extensive case studies on the 140-bus Northeast Power Coordinating Council (NPCC) system [5] under various contingencies. Section VI discusses the trade-off between the two methods, and finally Section VII states the conclusion.

II. PROBLEM FORMULATION

For a reliability coordinator (RC), the entire interconnection can be partitioned into an internal system (InSys) and an external system (ExSys). An RC usually has both accurate dynamic models and real-time observability for InSys, but not ExSys. In reality, there may be a cushion area where the RC has partial observability; however, in this paper, we consider it part of the ExSys as well. Take the 140-bus NPCC system as an example, InSys and ExSys, connected through two tie-lines [28], are illustrated in Fig. 1. Tie-lines are the connecting links between Insys and Exsys.

InSys (bus1-36), which is the simplified ISO New England (ISO-NE) system, represents the subsystem that can be characterized by precise knowledge of its structure and parameters, enabling a straightforward formulation using dynamic models for each component. The model-based InSys can be formulated based on the known dynamics of each component (e.g., the generators, turbines, exciters, loads, converter controls, transmission lines) by a set of DAE in (1a)-(1b).

In contrast, ExSys (bus37-140) lacks accessible physics models due to unavailable system state measurements, privacy concerns, and inaccessible local measurements, e.g.,real-time dispatch of the generators. The accessible state variables of Exsys are limited to those associated with tie lines, e.g., currents on tie lines. Therefore, a data-driven neural network-based dynamic equivalence is relied upon to model ExSys, as in (1c):

$$\begin{cases} \dot{x}_{in} = \mathcal{P}(x_{in}, y_{in}, i_{tie}) & \text{(1a)} \\ \mathcal{G}(x_{in}, i_{tie}, y_{in}) = 0 & \text{(1b)} \\ \dot{x}_{ex} = \mathcal{N}_\theta(x_{ex}, z_{in}) & \text{(1c)} \end{cases}$$

Here, x_{in} denotes the state variables of InSys's components (e.g., generators, turbines, exciters); y_{in} denotes the algebraic variables of InSys such as power flow states; i_{tie} denotes the currents flowing through the tie-lines. Functions $\mathcal{P}$ and $\mathcal{G}$ denote the dynamic and algebraic equations of InSys, respectively, which can be readily established based on the physics models of InSys.z_{in} denotes the features from InSys, which is selected from part of the states of InSys to describe the interaction between InSys' dynamics and ExSys' dynamics. x_{ex} denotes the state variables of ExSys, the tie-line currents. $\mathcal{N}$ is the forward propagation function of a neural network. The objective is to learn such a $\mathcal{N}$ that reflects the ExSys dynamics. The outputs are the derivatives of the tie-line currents, denoted by $\dot{x}_{ex}$. This neural network is multi-layer structured, whose forward propagation can be functionally expressed as:

$$\mathcal{N}(x_{ex}, z_{in}) = \mathcal{L}_m(\mathcal{L}_{m-1}(\cdots \mathcal{L}_1(x_{ex}, z_{in}, \theta_1)\cdots, \theta_{m-1}), \theta_m) \quad (2)$$

where $\mathcal{L}_m$ denotes the loss function of the m^{th} layer and θ_m denotes the corresponding weights in that layer. The universal

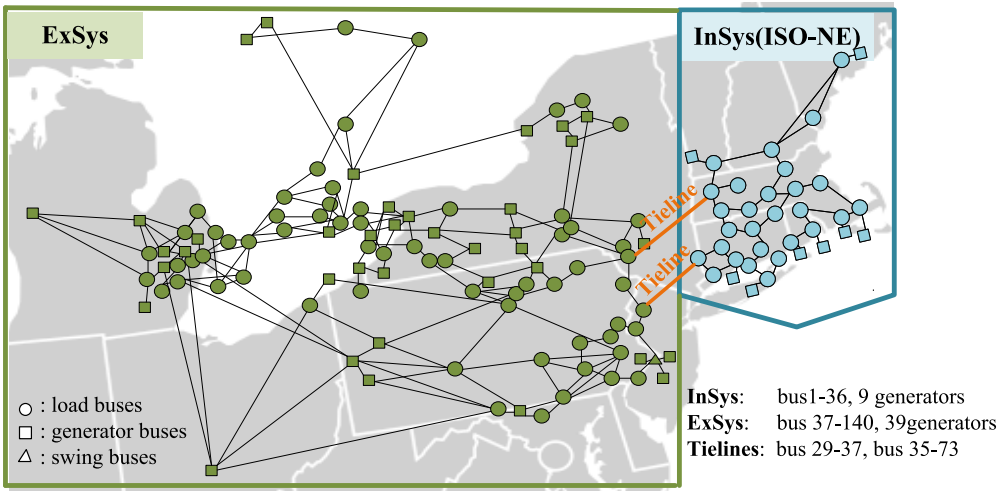

FIGURE 1. Topology of the NPCC system.

approximation theorem ensures that a neural network with 1 hidden layer can approximate any continuous functions for inputs within a specific range. Therefore, the advantage of a neural network-enabled dynamic equivalence lies in its flexibility for approximating a dynamic system without requiring the system to be linear or assuming any dynamical modes beforehand.

III. ODE-NET-ENABLED DYNAMIC EQUIVALENCE

A neural network can be conceptualized as a nonlinear function governed by parameters denoted as θ. Within the realm of machine learning, these parameters are optimized by minimizing a loss function, conventionally determined as the disparity between observed measurements and the corresponding outputs of the neural network. This equivalencing problem is formulated as an ordinary differential equation to represent the state space model. The challenge in this particular context stems from the neural network output being the derivative of x_{ex}, while the available measurements only provide x_{ex}, as in (1b). Consequently, the direct construction of a loss function becomes inherently infeasible. In addressing this predicament, two distinct approaches present themselves: discrete-time learning and continuous-time learning.

A. NECESSITY OF CONTINUOUS-TIME LEARNING

Conventional machine learning techniques for dynamic equivalence primarily rely on discrete-time learning. In discrete-time learning, the loss function for neural network training is usually constructed by discretizing the continuous-time differential equations into discrete-time difference equations. For example, based on the trapezoidal rule, the ExSys dynamics can be discretized as:

$$\frac{x_{ex}(t)-x_{ex}(t-\Delta)}{\Delta} = \frac{1}{2}[\mathcal{N}(x_{ex}(t), z_{in}(t)) + \mathcal{N}(x_{ex}(t-\Delta), z_{in}(t-\Delta))] \quad (3)$$

Correspondingly, the loss function can be established, and the neural network can be optimized by:

$$\begin{aligned} &min_\theta \sum_{i=0}^{n} L_{discrete} = \sum_{i=0}^{n} \frac{1}{2}\eta_i ||y_i - \hat{y_i}||_2 \\ &s.t.\ \ \hat{y} = \frac{1}{\Delta}(\hat{x}_{ex}(t) - \hat{x}_{ex}(t-\Delta)) \\ &y = \frac{1}{2}[\mathcal{N}(x_{ex}(t), z_{in}(t)) + \mathcal{N}(x_{ex}(t-\Delta), z_{in}(t-\Delta))] \end{aligned} \quad (4)$$

where the subscript i denotes the time-step, n is the number of total time steps, $\hat{y}$ denotes the derivatives estimated from the measurements; and y denotes the derivatives estimated from the neural network; η_i denotes the weighting factor at time step i.

However, this approach is sensitive to derivative estimation, resulting in biased training due to accumulated residue errors during training or non-ideal measurements. Although discrete-time training may produce satisfactory derivatives fitting, it cannot guarantee the accuracy of system states after numerical integration, leading to unsatisfactory performance in learning continuous-time dynamics.

In contrast, our solution is an ODE-NET-enabled dynamic equivalence, which adopts a continuous-time learning philosophy by directly minimizing the error between the state measurements $\hat{x}$ and the numerical solution of (2):

$$\begin{aligned} &\min_\theta \sum_{i=0}^{n} L(x_{ex,i}) = \sum_{i=0}^{n} \frac{1}{2}\eta_i ||x_{ex,i} - \hat{x}_{ex,i}||_2 \\ &s.t.\ \ \frac{dx_{ex}}{dt} = \mathcal{N}(x_{ex}, \hat{z}_{in}, \theta) \end{aligned} \quad (5)$$

Comparing (5) with (4), an obvious distinction is that ODE-NET is capable of directly minimizing the difference between real dynamic states and trained dynamic states, which requires no discretization and fully respects the continuous-time characteristics of power system dynamics. Therefore, it is theoretically less vulnerable to non-ideal measurements and residue training errors.

B. PHYSICS-INFORMED CONTINUOUS BACK PROPAGATION

Traditional DNNs are generally trained by backpropagation, which computes the gradient of the loss function to the DNN parameters at each layer to update the DNN. However, the ODE-NET training shown in (5) differentiates from the conventional loss function, such as (4). Because it involves numerical integration in its constraints.

To deal with the integration-incorporated constraints, ODE-NET adopts a continuous backpropagation technique to train the network. An adjoint method [7] is introduced to transform (5) into a format that removes the numerical integration constraints; then a physic-informed (PI) continuous-backpropagation technique is developed as follows:

$$\begin{aligned}
&\min_\theta \sum_{i=0}^{n} L_i = \sum_{i=0}^{n} \frac{\eta_i}{2}(||x_{ex,i} - \widehat{x}_{ex,i}||_2 + ||x_{in,i} - \widehat{x}_{in,i}||_2) \\
&\mathcal{L} = \sum_{i=0}^{n} L_i - \int_{t_0}^{t_n} \left[\lambda^T(\dot{x}_{ex} - \mathcal{N}_\theta) + \mu^T(\dot{x}_{in} - \tilde{\mathcal{P}})\right] dt \\
&s.t.\ \ x_{ex,i} = \widehat{x}_{ex,0} + \int_{t_0}^{t_i} \mathcal{N}(x_{ex}, z_{in}, \theta) dt \\
&\qquad x_{in,i} = \widehat{x}_{in,0} + \int_{t_0}^{t_i} \tilde{\mathcal{P}}(x_{in}, y_{in}, i_{tie}) dt
\end{aligned} \tag{6}$$

where λ and μ respectively denote the adjoint states for ExSys and InSys, $\tilde{\mathcal{P}}$ is equivalently formulated from (1). A dynamic equivalence is theoretically non-autonomous, where the InSys' states also impact the ExSys' dynamics. Consequently, both the dynamics of InSys and ExSys are incorporated into (6), ensuring the effectiveness of ODE-NET in simulating the closed-loop dynamics of the entire power system. Utilizing appropriate adjoint boundary conditions [7], the physics-informed gradient is expressed as follows:

$$\frac{d}{dt}\begin{bmatrix} \lambda^T \\ \mu^T \\ \partial\mathcal{L}/\partial\theta \end{bmatrix} = \begin{bmatrix} -\lambda^T \partial\mathcal{N}/\partial\, x_{ex} - \mu^T \partial\tilde{\mathcal{P}}/\partial\, x_{ex} \\ -\lambda^T \partial\mathcal{N}/\partial\, x_{in} - \mu^T \partial\tilde{\mathcal{P}}/\partial\, x_{in} \\ \lambda^T \partial\mathcal{N}/\partial\, \theta \end{bmatrix} \tag{7}$$

Finally, the gradient descent for $\mathcal{N}_\theta$ can be performed using $\partial\mathcal{L}/\partial\theta|_{t=0}$ integrated from (7) by any ODE solvers (the integration operation). θ is updated according to:

$$\theta^* \leftarrow \theta - \frac{\partial\mathcal{L}}{\partial\theta} \tag{8}$$

As illustrated in Fig. 2, (6) explicitly embeds the accuracy of both ExSys and InSys states in a closed-loop manner, which ensures NeuDyE generates dependable dynamic responses in conformance with the system's real dynamics once the training converges.

IV. SEEN FROM DRIVING PORT EQUIVALENCE

In the previously formulated Physics Informed NeuDyE (PI-NeuDyE), optimal closed-loop outcomes are attained

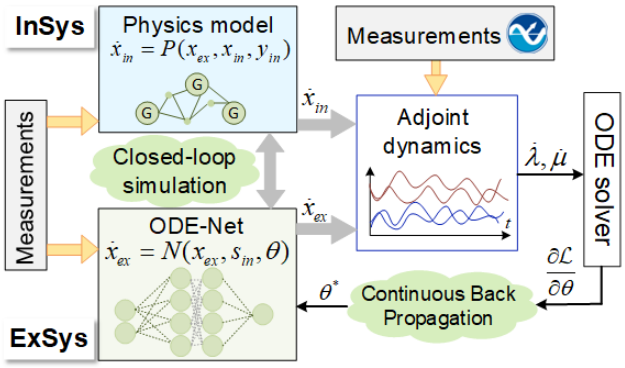

FIGURE 2. Physics-informed NeuDyE.

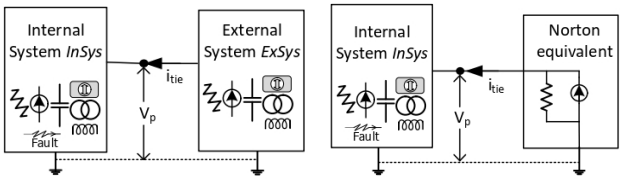

(a) Original networks. (b) Norton equivalent network.

FIGURE 3. Driving port dynamic equivalence.

through sufficient internal system inputs, which may not be readily accessible in practical applications [27]. Another concern is that the PI-NeuDyE while considering the interaction between the ExSys and InSys in a closed-loop manner, ensures testing accuracy at the expense of compromised training efficiency. To address these limitations and enhance the method's applicability in real-world scenarios, we introduce a more scalable neural equivalent technique known as the Driving Port (DP) NeuDyE. This novel approach necessitates only the knowledge of boundary voltages on the tie-lines, thereby facilitating the practical implementation of NeuDyE in utility and industrial systems.

A. ALGEBRAIC COMPONENT SEPARATION

To form the neural network-integrated power grid, the following equations (1), the selection of x_{ex} and z_{in} is necessary. If the topology of ExSys is static, it can be substituted with a Norton equivalent current source, illustrated in Fig. 3b. From the standpoint of InSys, whether ExSys is represented in full detail, as depicted in Fig. 3a, or as a Norton equivalent current source, as shown in Fig. 3b, both representations yield the same output i_{tie} for a given input v_p. Inspired by the Norton equivalent theory, a neural network observed from the driving port is devised.

To capture its nonlinear dynamics, measurements of port voltages v_p and tie-line currents i_{tie} are utilized to discover the state space model of ExSys as shown in Fig. 3. The tie-line currents i_{tie} are selected as the state variables x_{ex} for the external system, whose continuous differential structure is represented by the neural network; then the algebraic component separation is introduced below:

$$\begin{cases} \dfrac{di_{tie}}{dt} = \mathcal{N}(i_{tie}, v_p, \theta) \\ \mathcal{G}(i_{tie}, v_p) = 0 \end{cases} \tag{9}$$

where the port voltages v_p corresponds to the InSys features z_{in} in (1c). The tie-line currents i_{tie} can then be represented as a linear combination of state variables and inputs:

$$i_{tie} = C_s \cdot x_{ex} + D \cdot v_p \tag{10}$$

where matrices C_s and D are constant matrices. If a fault happens in InSys at time instant t_i, sudden changes may happen in $\Delta v_p(t_i) = v_p(t_i + \Delta t) - v_p(t_i)$, while $x_{ex}(t_i)$ keeps invariant in a very short period of Δt, i.e. $\Delta x_{ex}(t_i) = 0$. The components i_{tie} can be split into two types of components: continuous-state-variable components $i_{tie\_cs} = C_s \cdot x_{ex}$ and algebraic components $i_{tie\_a} = D \cdot v_p$.

On one hand, algebraic components embody the immediate contribution from the port voltages, which may exhibit discontinuity during switching events within the internal network. On the other hand, continuous-state-variable components, i_{tie_cs}, are employed as the constituents of the neural network equivalent, fulfilling the requirement for continuity as depicted in equation (9).

To compute the coefficient matrix D, we leverage measurements obtained during the fault period via the least squares method, as shown below:

$$\begin{bmatrix} D_{11} & \cdots & D_{1n_p} \\ \vdots & \ddots & \vdots \\ D_{n_p1} & \cdots & D_{n_pn_p} \end{bmatrix} = \left[\Delta i_{tie}(t_1), \cdots, \Delta i_{tie}(t_{n_f})\right] \cdot \left[\Delta v_p(t_1), \cdots, \Delta v_p(t_{n_f})\right]^{-1}$$

where n_p is the number of port voltages and n_f is the number of faults whose port voltages and tie-line currents are recorded in the data sets. Define $\Delta v_p(t_i) = v_p(t_i + \Delta t) - v_p(t_i)$ and $\Delta i_{tie}(t_i) = i_{tie}(t_i + \Delta t) - i_{tie}(t_i)$. The continuous component i_{tie_cs} can then be extracted as:

$$i_{tie\_cs} = i_{tie} - D \cdot v_p \tag{11}$$

The neural equivalent network in (9) and the DAE now become:

$$\begin{cases} \dfrac{di_{tie\_cs}}{dt} = \mathcal{N}(i_{tie\_cs}, v_p, \theta) \\ \dfrac{dx_{in}}{dt} = \mathcal{P}(x_{in}, y_{in}, i_{tie}) \\ \mathcal{G}(x_{in}, y_{in}, i_{tie\_cs}, i_{tie}, v_p) = 0 \end{cases} \tag{12}$$

The neural equivalent of the external system and the corresponding formulated interface, as shown in Fig. 4, are integrated into the transient stability simulation. The equivalent admittance is formed by the coefficient matrix (admittance matrix) in (11). The values of current sources are updated by applying an explicit integration to (12).

B. FORMULATION OF ODE-NET BASED DRIVING PORT EQUIVALENCE

As aforementioned, measurements are inherently discrete in real-world power networks, even though the underlying system is continuous. Therefore, DP-NeuDyE is again discovered through a continuous-time learning manner,

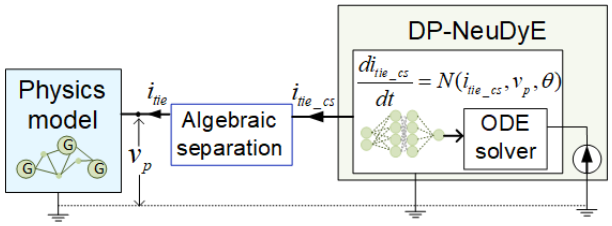

FIGURE 4. DP-NeuDyE with algebraic separation.

as depicted in (12), from discrete measurements i_{tie} and v_p. During the time interval $[0, t_n]$, DP-NeuDyE is trained by minimizing the loss function defined by the error between the state measurements $\hat{i}_{tie\_cs}$ and the numerical solution i_{tie_cs} by (12), as illustrated below:

$$L = \sum_{i=0}^{n} \frac{1}{2} ||i_{tie\_cs}(t_i) - \hat{i}_{tie\_cs}(t_i)||_2 \tag{13}$$

where $i_{tie\_cs}(t_i) = \widehat{i}_{tie\_cs}(0) + \int_0^{t_i} \mathcal{N}(x, u, \theta)dt$.

Similar to (7), the challenge in minimizing (13) stems from the integration operation in the constraints. DP-NeuDyE again tackles this challenge by treating the ODE solver as a black box and computing gradients using the adjoint sensitivity method [8].

C. STRENGTHENING DP-NEUDYE VIA RECURRENT NEURAL NETWORK

Data-driven methodologies predominantly depend on observable states to construct the neural equivalent model, as exemplified in (12). However, this model reduction approach inherently leads to a scenario where state variables constitute only a minor subset of the comprehensive state variables present in the original power network. As a result, such a reduction may not entirely encapsulate all the crucial dynamic properties intrinsic to the power system. To address this deficiency of training features, DP-NeuDyE is enhanced by leveraging historical data through the implementation of Recurrent Neural Networks (RNNs), effectively expanding the dataset by incorporating past information. RNNs, with their unique ability to remember past information, provide a robust mechanism to incorporate temporal dynamic behavior into the model [9], thereby improving the model's performance under insufficient training data. The integration of RNNs into the DP-NeuDyE framework is illustrated in Fig. 5 and explained as follows.

As illustrated in Fig. 5, within a specific neuron, the RNN cell integrates the output of this neuron from previous time steps into the computation of the current time step's output. This mechanism effectively leverages historical data from the preceding time step to assist in calculating the output of the current time step. Thus, RNN ameliorates potential information deficiencies that might arise when computations rely on a limited subset of state variables, thereby bolstering the overall accuracy and robustness of DP-NeuDyE.

Similar to Section III, the backward propagation should be used to calculate the gradient of the neural network

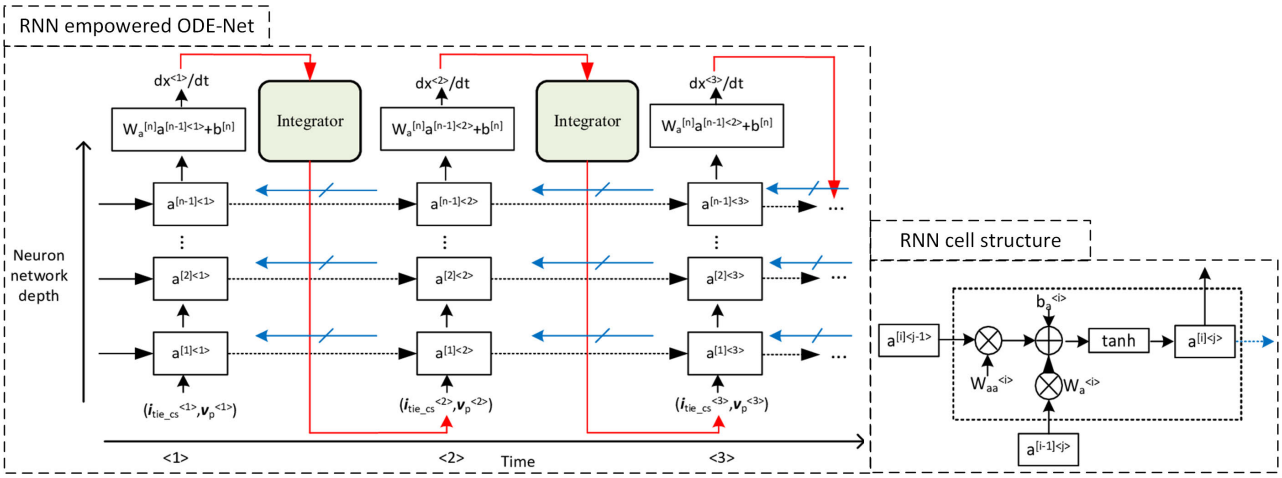

FIGURE 5. RNN-empowered DP-NeuDyE.

parameters. Recall that the continuous backpropagation in Subsection IV-B already considers integration along the time by solving an augmented differential equation. Therefore, the backward propagation throughout time for the RNN cell is ignored and the gradient descent method used in Subsection IV-B can directly be applied to the RNN-empowered DP-NeuDyE.

V. TEST RESULTS

In this section, the detailed training and testing procedures of NeuDyE are introduced. Simulation results of PI-NeuDyE and DP-NeuDyE are presented to demonstrate their efficacy and practicality.

A. ALGORITHM SETTINGS

The ground truth electromechanical trajectories are obtained by simulating the complete, physics-based 140-bus NPCC system via the Power System Toolbox (PST) [10]. The PST results are verified with simulations from the Transient Security Assessment Tool (TSAT). The trapezoidal rule is adopted as the numerical integration method.

1) NEUDYE TRAINING

PI-NeuDyE: as introduced in Section III, the selected states are from generators, exciters, governors, and line currents of InSys as s_{in}, in total 90 dimensions; the currents flowing in the two tie-lines are the states x_{ex} of ExSys. Notably, such training features can be flexibly adjusted according to available measurements.

DP-NeuDyE and RNN-DP-NeuDyE: followed by IV, s_{in} includes boundary voltages with 4 dimensions (2 tie-lines, each with a real part and an imaginary part); x_{ex} consists of tie-line currents.

2) NEUDYE TESTING

Once an ODE-NET is acquired, its performance is evaluated through closed-loop tests. In the closed-loop context, the ODE-NET-based ExSys model takes the place of the large and unknown external systems. This neural equivalent Exsys model integrates with the physics-based InSys model, forming a physics-neural-integrated system that operates as a unified whole. This constitutes the final setup, where the dynamics of the entire system are computed through numerical integration.

The predicted values are trajectories simulated by the physics-neural-integrated system, which contains the 36-bus, physics-based InSys and the ODE-NET-based dynamic equivalence of the ExSys, representing the remaining 104 buses. If the NeuDyE can accurately mimic the dynamics of the original ExSys, the predicted values from the physics-neural-integrated system should be close to the true values, i.e., simulation with the full physical system model.

B. SIMULATION RESULTS

1) VALIDITY OF PI-NEUDYE UNDER VARIOUS FAULT CLEARING TIMES AND FAULT LOCATIONS

As mentioned in Section III, traditional discrete learning may yield satisfactory predictions in open-loop training by fitting the derivatives, as in Fig. 6a, which is the prediction from a DNN. Whereas in the closed-loop test in Fig. 6b, DNN fails to capture the continuous dynamics after the integration. The biased training emerges from accumulated residue errors during the training process. Even though the discrete-learning DNN yields flawless predictions of derivatives in the open-loop training, during the testing, where the DNN works with Insys in a closed loop to output the final results, the integrated results are impractical. This underscores the imperative for continuous learning.

Depicted in Fig. 7, 25 training scenarios are generated by launching three-phase faults at 0.50s at bus 18, 19, 20, 21, or 28 with fault clearing randomly within a time interval [0.53s, 0.6s]. The training variables of InSys have 90 dimensions as mentioned in V-A.

Fig. 8 shows the closed-loop test results of boundary voltages with faults on bus 21 cleared at 0.5405s, and 0.6108s, which are new values to the training sets. The perfect match

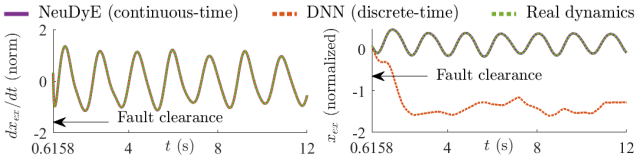

(a) Open-loop training performance. (b) Closed-loop testing performance.

FIGURE 6. Comparison of NeuDyE with conventional discrete-time DNN.

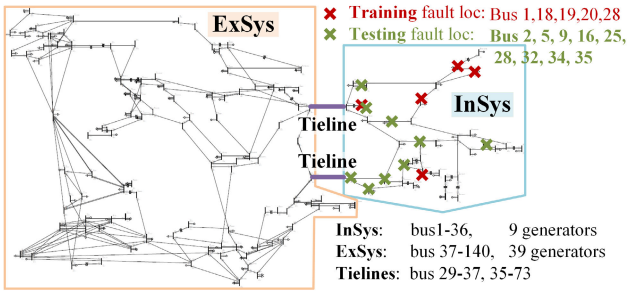

FIGURE 7. 140-bus NPCC system training and testing locations.

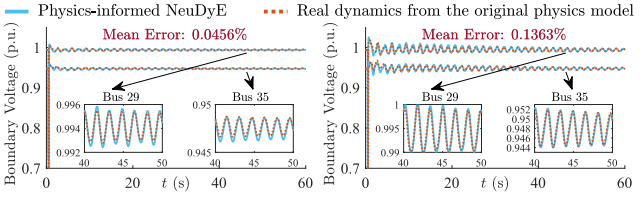

(a) Fault cleared at 0.5405s. (b) Fault cleared at 0.6108s.

FIGURE 8. Accuracy of PI-NeuDyE under a fault at bus 21.

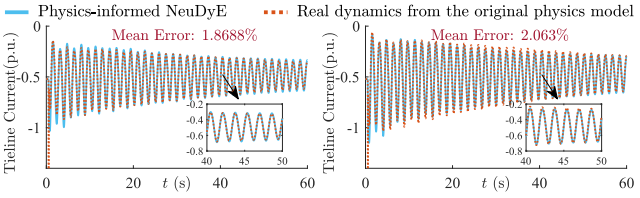

(a) Fault at bus 5 cleared at 0.58s. (b) Fault at bus 32 cleared at 0.58s.

FIGURE 9. Accuracy of PI-NeuDyE under different fault locations.

illustrates the accuracy of the developed method under varied fault clear times. In Fig. 9, test results of tie-line currents with faults on bus 5 and bus 32 demonstrate a perfect match between PI-NeuDyE's results and that from the full NPCC model.

Further, 108 testing scenarios are generated with new fault locations and random fault clearing times at bus 2, 5, 9, 16, 25, 28, 32, 34 and 35. Fig. 10 presents that the overall relative error is lower than 1%, indicating a satisfying generalization ability. Fig. 8-10 show that the derived PI-NeuDyE model can properly and accurately represent the dynamics and transients, regardless of changes in fault durations or fault locations.

As mentioned in Subsection V-A, choosing features of InSys is flexible. Other settings, like using active and reactive power of transmission lines or bus voltages and line currents, are also feasible. As an example, Fig. 11a presents a new testing result by using boundary voltages between ExSys and InSys and all branch currents in InSys as training features

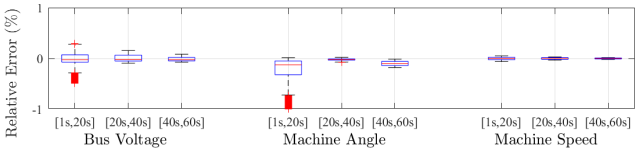

FIGURE 10. Accuracy of PI-NeuDyE under new scenarios.

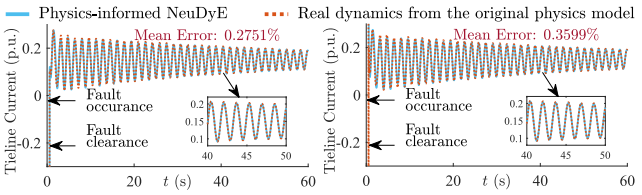

(a) Features: all branch currents and boundary voltages. (b) Features: boundary currents and all voltages.

FIGURE 11. Performance of NeuDyE using other measurements.

(90 dimensions for InSys). Fig. 11b uses boundary currents and voltage from all buses (76 dimensions for InSys). The fault clears at 0.56s on bus 2. The predicted trajectories match with the measurements closely, with a mean error of less than 0.3%, indicating high accuracy and satisfactory performance of NeuDyE using different settings of training features.

A noteworthy observation from the simulation results is the presence of low-damping oscillations. It is observable that even after 60 seconds, the tie-line currents and boundary voltages still have small oscillations. This is attributed to the inter-area modes of the NPCC system, as extensively discussed in [28] and [29]. The system's eigenvalues possess extremely small real parts, resulting in intrinsic low-damping dynamics. This characteristic necessitates the Neural Network (NN) to exhibit both a long total simulation time to capture the slow dynamics and a small time step to grasp the fast transients simultaneously, presenting a formidable challenge for any NN to learn. The demonstrated efficacy of NeuDyE in capturing both the swift oscillations and the gradual damping tendency highlights its versatility in handling stiff systems characterized by multi-time-scale dynamics. This capability positions NeuDyE as a promising solution for systems with intricate and challenging temporal dynamics.

2) REDUCED VARIABLES USING DP-NEUDYE

As previously mentioned, DP-NeuDyE is designed for potential practical applications that require limiting the number of input variables. In contrast with Subsection V-B1, where the number of InSys features used in Fig. 8 and Fig. 11 are 90 or 76 dimensions, DP-NeuDyE only needs 4 dimensions of InSys features. The selection of ExSys features is the same for both methods. The ExSys subsystem, as depicted in Fig. 1, is modeled by the DP-NeuDyE as illustrated in Fig. 4. The training trajectories are derived from faults happening in five distinct buses, each triggered by phase-to-ground faults at the T-line, as highlighted in red in Fig. 12. All the faults occur at 0.5s and clear at 0.55s. The testing locations are shown in green.

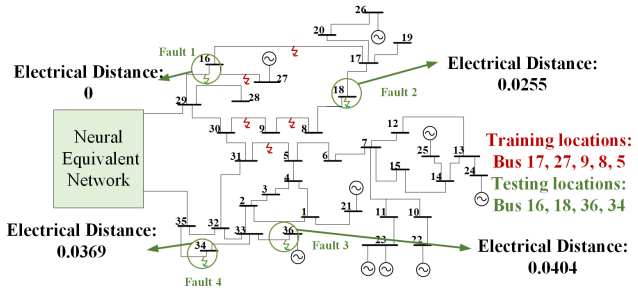

FIGURE 12. Training and testing locations for DP-NeuDyE.

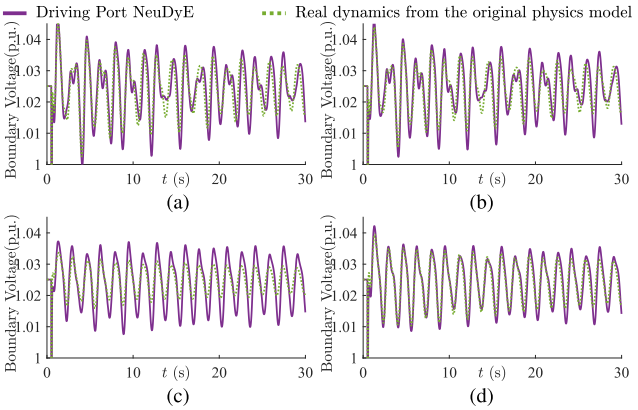

FIGURE 13. Testing results of DP-NeuDyE.

In Fig. 13, it is evident that DP-NeuDyE adeptly predicts low-frequency oscillations across a considerable domain. The ability to precisely forecast scenarios beyond the training set serves as validation for the efficacy of the proposed method. Furthermore, the full model-based trajectory exhibits two oscillation modes: one at 0.5991 Hz with a magnitude of 0.2155 and another at 1.24813 Hz with a magnitude of 0.1349. The simulation based on the neural equivalent model also accurately predicts these oscillation modes, with magnitudes of 0.2051 and 0.1431, respectively.

3) GENERALIZABILITY ANALYSIS BASED ON ELECTRICAL DISTANCE

To quantify the NeuDyE models' generalization performance, the electrical distance is employed between the fault locations in the testing set and those in the training set as a measure. The network topology is transformed into an adjacency matrix using graph theory, as depicted below, thereby establishing an automated method for predicting the performance of the introduced neural ODE model for subsystems. Consequently, the electrical distance between a new fault location and those in the training set can be determined from the adjacency matrix A by selecting the shortest distance.

$$A = \begin{cases} \text{Electric connection between Bus } i \text{ and } j\text{: } A_{ij} = X_{ij} \\ \text{Else: } A_{ij} = 0 \\ \text{Fault dynamic record near Bus } i\text{: } A_{ii} = 1 \end{cases}$$

In the previous case study as depicted in Fig. 12, the electrical distances from the test set to the training set are as follows: 0, 0.0255, 0.0404, 0.0369. These electrical distances are relatively small; the generalizability of the DP-NeuDyE is thus relatively good. In terms of the performance in predicting boundary voltage, Fig. 13c is already not satisfiable compared with results from PI-NeuDyE in Fig. 8 and in Fig. 10. If a fault occurs at a considerably remote distance from those in the training set, such as the T-line between bus 19 to 17, where the electrical distance is 0.0948, DP-NeuDyE may output divergent dynamic predictions as in Fig. 14a. Even though RNN-empowered DP-NeuDyE yields convergent results in Fig. 14a, it still faces challenges in achieving precision.

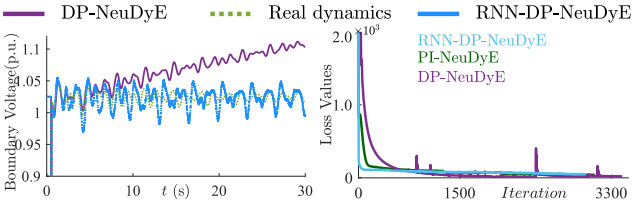

(a) Testing results of DP-NeuDyE under distant fault. (b) Loss reduction over training iterations.

FIGURE 14. Comparison among DP-NeuDyE, RNN-DP-NeuDyE and PI-NeuDyE.

TABLE 1. Training time for different methods.

Method	Training time/ iteration	Total iters till convergence
PI-NeuDyE	49.1706s	3127
DP-NeuDyE	20.4417s	3322
RNN-DP-NeuDyE	103.2257s	2772

VI. DISCUSSION

From Table 1 and Fig. 14b, for the same training set, it is obvious that DP-NeuDyE is more efficient. The primary advantage of DP-NeuDyE lies in its ability to perform dynamic equivalence even with limited features in InSys. It is noteworthy that DP-NeuDyE utilizes only 6% of the inputs compared to PI-NeuDyE. This capability eliminates the requirement for extensive data acquisition and storage resources. However, the increased training time for RNN-empowered DP-NeuDyE is notable. This is attributed to the RNN-ODE-Net for training, while PI-NeuDyE and DP-NeuDyE employ ODE-Net with a Multilayer Perceptron (MLP) structure. The inherently slower training speed of RNN compared to MLP, even with the same network size, contributes to the observed increase in training time.

Another observation is DP-NeuDyE offers advantages particularly when dealing with highly limited training sets. However, its performance is not as commendable as PI-NeuDyE for faults occurring from a large electrical distance. The primary reason behind this discrepancy lies in the training process. PI-NeuDyE trains in a closed-loop manner by considering the interacting dynamics of both InSys and ExSys, involving 90 dimensions of InSys features. Whereas DP-NeuDyE only sees from the driving port, utilizing only 4 dimensions of boundary measurements as InSys features. As a result, there exists a trade-off

between training efficiency and generalization ability, which impacts the performance of the DP-NeuDyE for faults in distant areas. Even though the utilization of RNN can improve the generalization capability of DP-NeuDyE, further investigation is required to address its time-consuming nature of training.

To summarize, for faults not too distant from the training sets, both DP-NeuDyE and PI-NeuDyE yield satisfactory results. In cases where a fault is significantly distant from the training set, PI-NeuDyE remains effective, while DP-NeuDyE proves inadequate unless the training set is expanded across a wider area. Balancing data size and diversity with model complexity is crucial, requiring more diversified data for robust generalization.

VII. CONCLUSION AND FUTURE WORK

This article proposes an ODE-Net-enabled Neural Dynamic Equivalence and its variants, PI-NeuDyE and DP-NeuDyE, which uncovers a powerful continuous-time dynamic equivalence of external systems. Their effectiveness is demonstrated on the 140-bus NPCC system, showcasing their performances under diversified scenarios. The scalable NeuDyE methods show that neural models can handle large-scale and complicated dynamical systems, which is essential for real-world power system applications with varying dynamics.

In the future, the authors aim to enhance method efficiency by incorporating advanced computing technologies, sparsity techniques for power grid formulation, and time-domain simulation.

REFERENCES

[1] M. L. Ourari, L.-A. Dessaint, and V.-Q. Do, "Dynamic equivalent modeling of large power systems using structure preservation technique," *IEEE Trans. Power Syst.*, vol. 21, no. 3, pp. 1284–1295, Aug. 2006.

[2] Y. G. I. Acle, F. D. Freitas, N. Martins, and J. Rommes, "Parameter preserving model order reduction of large sparse small-signal electromechanical stability power system models," *IEEE Trans. Power Syst.*, vol. 34, no. 4, pp. 2814–2824, Jul. 2019.

[3] I. Tyuryukanov, M. Popov, M. A. M. M. van der Meijden, and V. Terzija, "Slow coherency identification and power system dynamic model reduction by using orthogonal structure of electromechanical eigenvectors," *IEEE Trans. Power Syst.*, vol. 36, no. 2, pp. 1482–1492, Mar. 2021.

[4] N. Tong, Z. Jiang, S. You, L. Zhu, X. Deng, Y. Xue, and Y. Liu, "Dynamic equivalence of large-scale power systems based on boundary measurements," in *Proc. Amer. Control Conf. (ACC)*, Jul. 2020, pp. 3164–3169.

[5] Y. Lei, Y. Liu, G. Kou, B. Wang, C. Li, K. Sun, Y. Liu, K. Tomsovic, and J. Chow, "A study on wind frequency control under high wind penetration on an NPCC system model," in *Proc. IEEE PES Gen. Meeting Conf. Exposit.*, Jul. 2014, pp. 1–5.

[6] D. Dylewsky, X. Yang, A. Tartakovsky, and J. N. Kutz, "Engineering structural robustness in power grid networks susceptible to community desynchronization," *Appl. Netw. Sci.*, vol. 4, no. 1, pp. 1–14, Dec. 2019.

[7] Y. Zhou and P. Zhang, "Neuro-reachability of networked microgrids," *IEEE Trans. Power Syst.*, vol. 37, no. 1, pp. 142–152, Jan. 2022.

[8] R. Chen, Y. Rubanova, J. Bettencourt, and D. Duvenaud, "Neural ordinary differential equations," 2019, *arXiv:1806.07366*.

[9] D. E. Rumelhart, G. E. Hinton, and R. J. Williams, "Learning representations by back-propagating errors," *Nature*, vol. 323, no. 6088, pp. 533–536, Oct. 1986.

[10] P. W. Sauer, M. A. Pai, and J. H. Chow, "Power system toolbox," in *Power System Dynamics and Stability: With Synchrophasor Measurement and Power System Toolbox*. IEEE Press, 2017, pp. 305–325, doi: 10.1002/9781119355755.ch11.

[11] T. Guo and J. V. Milanovic, "Online identification of power system dynamic signature using PMU measurements and data mining," *IEEE Trans. Power Syst.*, vol. 31, no. 3, pp. 1760–1768, May 2016.

[12] L. Zheng, W. Hu, Y. Zhou, Y. Min, X. Xu, C. Wang, and R. Yu, "Deep belief network based nonlinear representation learning for transient stability assessment," in *Proc. IEEE Power Energy Soc. Gen. Meeting*, Jul. 2017, pp. 1–5.

[13] T. Xiao, Y. Chen, S. Huang, T. He, and H. Guan, "Feasibility study of neural ODE and DAE modules for power system dynamic component modeling," *IEEE Trans. Power Syst.*, vol. 38, no. 3, pp. 2666–2678, May 2023.

[14] A. M. Stankovicc, A. T. Saric, and M. Milosevic, "Identification of nonparametric dynamic power system equivalents with artificial neural networks," *IEEE Trans. Power Syst.*, vol. 18, no. 4, pp. 1478–1486, Nov. 2003.

[15] H. Shakouri G. and H. R. Radmanesh, "Identification of a continuous time nonlinear state space model for the external power system dynamic equivalent by neural networks," *Int. J. Electr. Power Energy Syst.*, vol. 31, nos. 7–8, pp. 334–344, Sep. 2009.

[16] A. G. Parlos, K. T. Chong, and A. F. Atiya, "Application of the recurrent multilayer perceptron in modeling complex process dynamics," *IEEE Trans. Neural Netw.*, vol. 5, no. 2, pp. 255–266, Mar. 1994.

[17] C.-W. Liu, M.-C. Su, S.-S. Tsay, and Y.-J. Wang, "Application of a novel fuzzy neural network to real-time transient stability swings prediction based on synchronized phasor measurements," *IEEE Trans. Power Syst.*, vol. 14, no. 2, pp. 685–692, May 1999.

[18] S. Wen, Y. Wang, Y. Tang, Y. Xu, P. Li, and T. Zhao, "Real-time identification of power fluctuations based on LSTM recurrent neural network: A case study on Singapore power system," *IEEE Trans. Ind. Informat.*, vol. 15, no. 9, pp. 5266–5275, Sep. 2019.

[19] S. K. Azman, Y. J. Isbeih, M. S. E. Moursi, and K. Elbassioni, "A unified online deep learning prediction model for small signal and transient stability," *IEEE Trans. Power Syst.*, vol. 35, no. 6, pp. 4585–4598, Nov. 2020.

[20] Z. Shi, W. Yao, L. Zeng, J. Wen, J. Fang, X. Ai, and J. Wen, "Convolutional neural network-based power system transient stability assessment and instability mode prediction," *Appl. Energy*, vol. 263, Apr. 2020, Art. no. 114586.

[21] A. Gupta, G. Gurrala, and P. S. Sastry, "An online power system stability monitoring system using convolutional neural networks," *IEEE Trans. Power Syst.*, vol. 34, no. 2, pp. 864–872, Mar. 2019.

[22] M. Raissi, P. Perdikaris, and G. E. Karniadakis, "Physics-informed neural networks: A deep learning framework for solving forward and inverse problems involving nonlinear partial differential equations," *J. Comput. Phys.*, vol. 378, pp. 686–707, Feb. 2019.

[23] C. Moya and G. Lin, "DAE-PINN: A physics-informed neural network model for simulating differential algebraic equations with application to power networks," *Neural Comput. Appl.*, vol. 35, no. 5, pp. 3789–3804, Feb. 2023.

[24] J. Khazaei and F. Moazeni, "Model identification of distributed energy resources using sparse regression and Koopman theory," in *Proc. IEEE PES GTD Int. Conf. Exposit. (GTD)*, Istanbul, Turkiye, May 2023, pp. 33–38.

[25] B. Lusch, J. N. Kutz, and S. L. Brunton, "Deep learning for universal linear embeddings of nonlinear dynamics," *Nature Commun.*, vol. 9, no. 1, p. 4950, Nov. 2018.

[26] P. Sharma, V. Ajjarapu, and U. Vaidya, "Data-driven identification of nonlinear power system dynamics using output-only measurements," *IEEE Trans. Power Syst.*, vol. 37, no. 5, pp. 3458–3468, Sep. 2022.

[27] Q. Shen, Y. Zhou, Q. Zhang, S. Maslennikov, X. Luo, and P. Zhang, "Physics-aware neural dynamic equivalence of power systems," *IEEE Trans. Power Syst.*, vol. 39, no. 1, pp. 2341–2344, Jan. 2024.

[28] S. You, J. Guo, W. Yao, S. Wang, Y. Liu, and Y. Liu, "Ring-down oscillation mode identification using multivariate empirical mode decomposition," in *Proc. IEEE Power Energy Soc. Gen. Meeting (PESGM)*, Jul. 2016, pp. 1–5.

[29] A. M. Khalil and R. Iravani, "Impact of high-depth penetration of wind power on low-frequency oscillatory modes of interconnected power systems," *Int. J. Electr. Power Energy Syst.*, vol. 104, pp. 827–839, Jan. 2019.

[30] L. Cai, H. Yin, Y. Lan, T. Lan, X. Wu, H. Eckel, and H. Weber, "Sub-synchronous harmonic impedance analysis of doubly-fed induction generator wind turbine," *IFAC-PapersOnLine*, vol. 52, no. 4, pp. 165–169, 2019.

[31] A. T. Saric, M. T. Transtrum, and A. M. Stankovic, "Data-driven dynamic equivalents for power system areas from boundary measurements," *IEEE Trans. Power Syst.*, vol. 34, no. 1, pp. 360–370, Jan. 2019.

QING SHEN (Graduate Student Member, IEEE) received the B.S. degree in automation from Tianjin University, China, in 2019, and the M.S. degree in electrical and computer engineering from Columbia University, USA, in 2021. She is currently pursuing the Ph.D. degree with the Department of Electrical and Computer Engineering, Stony Brook University. Her research interests include power system dynamic and stability analysis, physics-informed machine learning, optimization, and control.

YIFAN ZHOU (Member, IEEE) received the B.S. and Ph.D. degrees in electrical engineering from Tsinghua University, Beijing, China, in 2014 and 2019, respectively. She has been a Postdoctoral Researcher with Stony Brook University, Stony Brook, NY, USA. She is currently an Assistant Professor with Stony Brook University. Her research interests include microgrid stability and control, formal methods, reachability analysis, and quantum computing.

PENG ZHANG received the Ph.D. degree in electrical engineering from The University of British Columbia, Vancouver, BC, Canada, in 2009. He is currently a Full Professor of electrical and computer engineering and a SUNY Empire Innovation Professor with Stony Brook University, Stony Brook, NY, USA. Previously, he was a Centennial Associate Professor and a Francis L. Castleman Associate Professor with the University of Connecticut, Storrs, CT, USA. He was a System Planning Engineer with BC Hydro and Power Authority, Canada, from 2006 to 2010. His research interests include AI-enabled smart grids, quantum-engineered power grids, networked microgrids, power system stability and control, cybersecurity, and formal methods and reachability analysis.

HUANFENG ZHAO (Member, IEEE) received the Ph.D. degree in electrical engineering from the University of Manitoba, Winnipeg, MB, Canada, in 2021. Sponsored by RTDS Technologies Inc., he held a position as a Postdoctoral Fellow with the University of Manitoba, from 2021 to 2022, with a focus on the efficient and precise EMT simulations of large-scale power systems. Subsequently, he was associated with Stony Brook University as a Research Scientist, from 2022 to 2023, working on advanced computational techniques for power system stability analysis and simulation. He is currently a Senior Power System Engineer with Nayak Corporation, with a focus on the simulation of modern power grids.

QIANG ZHANG (Senior Member, IEEE) is currently a Supervisor with the Emerging Technologies Team, ISO New England Inc. His major responsibilities include developing technology adoption strategies and roadmaps, and overseeing research and development in the areas of WAMS, IBR integration, EMT modeling and simulation, machine learning, and cloud computing.

SLAVA MASLENNIKOV (Senior Member, IEEE) received the M.S., Ph.D., and Doctor of Sciences degrees in power systems from Peter the Great St.Petersburg Polytechnic University, in 1979, 1984, and 1998, respectively. He is currently the Technical Manager of the Advanced Technology Solutions Department, ISO New England Inc., with a focus on research and development in areas of power system resilience, operations, stability, cascading analysis, synchrophasors, and smart grids.

XIAOCHUAN LUO (Senior Member, IEEE) is currently the Manager of the Power System Technology Group, ISO New England Inc. He is responsible for the technology strategy, research, and development of bulk power system operations and planning. He has more than eighty academic publications. He received the 2021 Energy Central Innovation Champion Award. He is the Vice Chair of the IEEE PES Working Group "Cloud4PowerGrid," IEEE Corporate Engagement Program (CEP) Liaison for ISO New England Inc., and the past Chair of the IEEE PES Technologies and Innovation Subcommittee.